Greenland Ice Sheet Contribution to 21st Century Sea Level Rise as Simulated by the Coupled CESM2.1-CISM2.1

Muntjewerf, Laura; Petrini, Michele; Vizcaino, Miren; Ernani da Silva, Carolina; Sellevold, Raymond; Scherrenberg, Meike D.W.; Thayer-Calder, Katherine; Bradley, Sarah L.; Lenaerts, Jan T.M.; More Authors

DOI
10.1029/2019GL086836

Publication date
2020

Document Version
Final published version

Published in
Geophysical Research Letters

Citation (APA)
Muntjewerf, L., Petrini, M., Vizcaino, M., Ernani da Silva, C., Sellevold, R., Scherrenberg, M. D. W., Thayer-Calder, K., Bradley, S. L., Lenaerts, J. T. M., & More Authors (2020). Greenland Ice Sheet Contribution to 21st Century Sea Level Rise as Simulated by the Coupled CESM2.1-CISM2.1. *Geophysical Research Letters*, *47*(9), Article e2019GL086836. https://doi.org/10.1029/2019GL086836

Geophysical Research Letters

RESEARCH LETTER
10.1029/2019GL086836

Special Section:
Community Earth System Model version 2 (CESM2) Special Collection

Greenland Ice Sheet Contribution to 21st Century Sea Level Rise as Simulated by the Coupled CESM2.1-CISM2.1

Laura Muntjewerf[1], Michele Petrini[1], Miren Vizcaino[1], Carolina Ernani da Silva[1], Raymond Sellevold[1], Meike D. W. Scherrenberg[1], Katherine Thayer-Calder[2], Sarah L. Bradley[3], Jan T. M. Lenaerts[4], William H. Lipscomb[2], and Marcus Lofverstrom[5]

[1]Department of Geoscience and Remote Sensing, Delft University of Technology, Delft, The Netherlands, [2]Climate and Global Dynamics Laboratory, National Center for Atmospheric Research, Boulder, CO, USA, [3]Department of Geography, The University of Sheffield, Sheffield, UK, [4]Department of Atmospheric and Oceanic Sciences, University of Colorado Boulder, Boulder, CO, USA, [5]Department of Geosciences, University of Arizona, Tucson, AZ, USA

Abstract The Greenland Ice Sheet (GrIS) mass balance is examined with an Earth system/ice sheet model that interactively couples the GrIS to the broader Earth system. The simulation runs from 1850 to 2100, with historical and SSP5-8.5 forcing. By the mid-21st century, the cumulative GrIS contribution to global mean sea level rise (SLR) is 23 mm. During the second half of the 21st century, the surface mass balance becomes negative in all drainage basins, with an additional SLR contribution of 86 mm. The annual mean GrIS mass loss in the last two decades is 2.7-mm sea level equivalent (SLE) year^{-1}. The increased SLR contribution from the surface mass balance (3.1 mm SLE year^{-1}) is partly offset by reduced ice discharge from thinning and retreat of outlet glaciers. The southern GrIS drainage basins contribute 73% of the mass loss in mid-century but 55% by 2100, as surface runoff increases in the northern basins.

Plain Language Summary The Greenland Ice Sheet (GrIS) gains mass at the surface from snowfall, and it loses mass from melting and runoff and from glacier calving at the ocean front. When these processes are in balance, the ice sheet does not contribute to global sea level change. Recent observations have shown that the ice sheet is losing mass and raising global mean sea level.

This study uses a global Earth system model that calculates ice flow of the GrIS, as well as processes in the atmosphere, ocean, land, and sea ice. For a modern reference, the model is forced with atmospheric greenhouse gas concentrations for the period 1850–2014. Next, the model is forced for the rest of the 21st century following the SSP5-8.5 scenario to study how the GrIS and the Earth system respond to a worst-case scenario.

By 2050, the GrIS loses mass that is equal to 23 mm of global mean sea level rise. During the second half of the 21st century, all regions of the GrIS lose mass because of increased surface melting and runoff, with the dry north playing a greater role. By 2100, the projected GrIS contribution to sea level rise is 109-mm sea level equivalent.

Key Points:
- CESM2.1-CISM2.1 simulates a 5.4 K global mean temperature increase and strong NAMOC weakening by 2100 in SSP5-8.5 w.r.t. preindustrial
- The Greenland Ice Sheet contributes 23 mm to global mean sea level rise by 2050 and 109 mm by 2100
- The role of the northern basins becomes more important as surface runoff strongly increases during the second half of the 21st century

Supporting Information:
- Supporting Information S1

Correspondence to:
L. Muntjewerf,
L.Muntjewerf@tudelft.nl

Citation:
Muntjewerf, L., Petrini, M., Vizcaino, M., Ernani da Silva, C., Sellevold, R., Scherrenberg, M. D. W., et al. (2020). Greenland Ice Sheet contribution to 21st century sea level rise as simulated by the coupled CESM2.1-CISM2.1. *Geophysical Research Letters*, *47*, e2019GL086836. https://doi.org/10.1029/2019GL086836

Received 24 DEC 2019
Accepted 20 MAR 2020
Accepted article online 9 APR 2020

1. Introduction

During the past two decades, the Greenland Ice Sheet (GrIS) has lost mass at an increasing rate (Shepherd et al., 2019) and has become a major contributor to global mean sea level rise (SLR) (Chen et al., 2017). The polar ice sheets were identified in the IPCC Fifth Assessment Report as large sources of uncertainty in 21st century SLR projections (Church et al., 2013). A recent expert assessment estimates that by 2100, the GrIS will contribute between 20- and 990-mm sea level equivalent (SLE), with a median of 230-mm SLE (Bamber et al., 2019). The uncertainty in SLR stems partly from insufficient understanding of the complex interactions and feedbacks among ice sheets, surface mass balance (SMB), and climate (Fyke et al., 2018), highlighting the importance of studies with coupled Earth system/ice sheet models (Goelzer et al., 2017; Vizcaino, 2014).

Many studies on future ice sheet evolution have been done using regional climate models with static ice sheet topography (Lenaerts et al., 2015; Rae et al., 2012; Tedesco & Fettweis, 2012) or dynamic ice sheet

models with prescribed climate forcing (e.g., Aschwanden et al., 2019; Graversen et al., 2011; Ruckamp et al., 2019). By accounting only for climate-SMB interactions or ice sheet-SMB interactions, these studies miss interactions between ice sheet dynamics and climate. Further, some studies with partially coupled ice sheet-climate models have used positive-degree-day schemes, which parameterize melt based on the number of days the temperature is above the melting point (e.g., Huybrechts et al., 2011; Mikolajewicz et al., 2007; Ridley et al., 2005;Vizcaino et al., 2008). In new climate regimes, however, empirical relations between melt and temperature may no longer hold, and an explicit surface energy balance (SEB) is necessary (Bauer & Ganopolski, 2017).

Physics-based models that explicitly resolve the SEB and snowpack processes are needed to simulate feedbacks, such as the ice-albedo feedback (Bougamont et al., 2007). A main challenge is the fine horizontal grid resolution needed to realistically simulate SMB gradients (Van den Broeke et al., 2008). There has been recent progress in coupling an SEB-based SMB calculation with ice dynamics using regional climate models of both intermediate complexity (Born et al., 2019; Krapp et al., 2017) and higher complexity (e.g., regional climate model MAR Le clec'h et al., 2019). However, the use of global models with SEB-based SMB to simulate Earth system interactions with ice sheets has been limited (Vizcaino et al., 2008, 2015).

In this study, the Community Earth System Model version 2 (CESM2 Danabasoglu et al., 2020) with an interactive GrIS model (CISM2.1 Lipscomb et al., 2019) is used to simulate the period 1850–2100 under historical and SSP5-8.5 forcing. The model includes an SEB-derived SMB calculation with multiple elevation classes (Fyke et al., 2011; Lipscomb et al., 2013; Sellevold et al., 2019) and, thus, is able to capture ice sheet-SMB-climate feedbacks. The simulations follow the protocols for coupled ice sheet-climate model experiments in the framework of the Ice Sheet Modeling Intercomparison Project for CMIP6 (ISMIP6 Nowicki et al., 2016). This paper presents the CESM2.1-CISM2.1 projection of 21st century global climate change and GrIS response, as well as the projected GrIS contribution to global mean sea level. Results are compared to CESM2.1 simulations without an interactive ice sheet.

2. Method: Model Description and Experimental Setup

2.1. The Community Earth System Model

The CESM2 (Danabasoglu et al., 2020) is a comprehensive, fully coupled Earth system model that is contributing simulations of past, present, and future climates to the Coupled Model Intercomparison Project phase 6 (CMIP6 Eyring et al., 2016). CESM2 includes component models of the atmosphere (CAM6), land (CLM5 Lawrence et al., 2019), ocean (POP2 Smith et al., 2010; Danabasoglu et al., 2012), sea ice (CICE5 Hunke et al., 2017), river transport (MOSART Li et al., 2015), and land ice (CISM2.1 Lipscomb et al., 2019). The simulations described here were run with nominal 1-degree horizontal resolution (~110 km at the equator) in the atmosphere, land, ocean, and sea ice components. The ice sheet model was run on a 4-km limited-area grid centered on Greenland.

2.2. Interactive Earth System/Ice Sheet Coupling

CESM2.1-CISM2.1 supports an evolving Greenland Ice Sheet that is interactively coupled to other Earth system components. The SMB is computed in CLM5 as the difference between annual snow accumulation and surface ablation, derived from the surface energy balance and snow pack hydrology. The SMB is calculated for multiple elevation classes in glaciated grid cells to account for subgrid-scale variations in surface climate and SMB components (Fyke et al., 2011; Lipscomb et al., 2013; Sellevold et al., 2019). The SMB is remapped from the CLM5 grid to the higher resolution CISM2 grid, using a trilinear interpolation scheme that conserves both the total ablated and the total accumulated mass (Leguy et al., 2018).

Freshwater fluxes from the GrIS to the ocean are the sum of surface runoff from CLM5 and basal meltwater and ice discharge from CISM2. Surface runoff is routed to the ocean via MOSART, accounting for the surface slope, and basal meltwater reaches the ocean by nearest neighbor routing. In the ocean, meltwater is distributed over the upper 30 m (Sun et al., 2017). Solid ice discharge (i.e., calving) is also routed to the nearest ocean neighbor but is spread diffusively in the ocean surface layer over a region extending up to 300 km from the coast and is melted instantaneously using energy from the ocean surface. Ocean thermal forcing to calving fronts is not simulated. Greenland's floating ice shelves, such as Petermann, are not simulated, and thus, the basal melt term refers only to grounded ice. This term is small compared to mass loss from surface runoff and calving and is disregarded in the remaining discussion.

Dynamic land units in CLM5 enable the transition from glaciated to non-glaciated land cover, consistent with the evolving ice sheet margin in CISM2. The ice sheet surface topography in CISM2 is used to recompute the glacier coverage in CLM5 at runtime, modifying the albedo, soil, and vegetation characteristics. Surface elevation and topographic roughness fields in CAM6 are updated every 10 years to incorporate ice sheet geometry changes in atmospheric calculations. The coupling is further described in the supporting information, Text S1.

2.3. Experimental Setup

We analyze two simulations: a historical run from 1850 to 2014 and its continuation to 2100 following the SSP5-8.5 scenario (Nowicki et al., 2016; O'Neill et al., 2016). The historical forcing is a reconstruction based on observations of greenhouse gas concentrations, stratospheric aerosol data (volcanoes), land use change, and solar insolation. The preindustrial (1850 CE) CO_2 concentration is 287 ppmv (parts per million by volume), increasing to 397 ppmv in 2014. Further details on the forcing protocol can be found in Eyring et al. (2016). The SSP5-8.5 scenario starts in 2015 at the end of the historical period and ends in 2100 when the atmospheric CO_2 concentration is 1,142 ppmv, and the radiative forcing is 8.5 W m^{-2} relative to preindustrial.

The initial condition of the historical simulation is the spun-up model state. A description of the spin-up procedure is provided in Text S2. At the beginning of our simulation, the GrIS is in near equilibrium with the simulated preindustrial climate of CESM2.1, with residual drift of about 0.03-mm SLE $year^{-1}$. This initial GrIS overestimates the present-day observed area and volume by about 15% and 12%, respectively.

2.4. Basin-Scale Analysis

For regional-scale analysis, we use six major Greenland drainage basins defined by Rignot and Mouginot (2012). The basins are directly remapped onto the CISM grid since the modeled drainage divide locations roughly agree with observations (see velocity fields of Figure S2a, showing observations from Joughin et al., 2010, 2015, and Figure S2b). In regions where the ice sheet extent is overestimated, drainage basins are extended to the ice sheet margin. By extending each drainage basin from the margin into the ocean based on the ice flow direction, we also define six major ice-ocean sectors that receive freshwater from each basin.

3. Results

The analysis focuses on three climatological periods: the contemporary period (average over 1995–2014) from the historical simulation and the mid-century (2031–2050) and end of century (2081–2100) from the SSP5-8.5 simulation.

3.1. Evolution of Global Climate and GrIS Mass Budget

The atmospheric CO_2 concentration increases from 287 ppmv in 1850 to 397 ppmv in 2014, 566 ppmv in 2050, and 1142 ppmv in 2100 (Figure 1, Table S1). The simulated end-of-century global mean near surface temperatures increase is 5.4 K relative to preindustrial. With respect to the contemporary period (1995–2014), the simulated global temperature increases by 1.4 K at mid-century and by 4.6 K at end of century. The Arctic amplification (AA) factor, defined as the ratio of temperature change north of 60°N to the global mean, is 2.0 by mid-century and 1.8 by end of century. The decrease in AA between mid-century and end of century is significant ($p < 0.01$) and is likely the result of reduced sea ice cover, since AA depends on the magnitude of sea ice change (e.g., Dai et al., 2019). At mid-century, sea ice concentration is still declining throughout the year, while at end of century, the Arctic is ice free in late summer and early fall and thus experiences no further loss.

The simulated North Atlantic Meridional Overturning Circulation (NAMOC; defined as the maximum of the overturning stream function north of 28°N and below 500 m depth in the North Atlantic basin) is relatively stable during the historical period, with a mean of 24 Sv (blue line in Figure 1b). The only exception is an anomalously stronger overturning circulation in the 1960s, when the NAMOC increases by about 3 Sv. RAPID-AMOC measurements at 26°N in the Atlantic basin give a mean overturning strength of 17 ± 3.3 Sv for 2000–2018 (Frajka-Williams et al., 2019), in good agreement with the simulated value (18.7 ± 2.4 Sv) at this latitude over the same period. During the 21st century, the simulated overturning cell progressively weakens, collapsing to 8.6 Sv by end of century (Table S3).

The simulated climate change drives a positive GrIS contribution to global mean SLR (Figure 1c). The rate of mass loss increases from the preindustrial near equilibrium (0.03-mm SLE $year^{-1}$) to 0.08-mm SLE $year^{-1}$ during the contemporary period, 0.55-mm SLE $year^{-1}$ by mid-century, and 2.68-mm SLE $year^{-1}$ by end

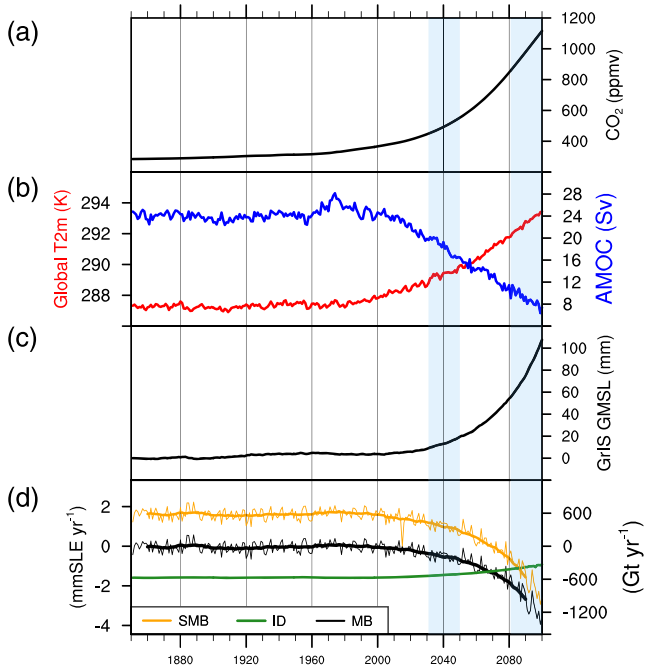

Figure 1. CESM2.1-CISM2.1 1850-2100 evolution of (a) CO_2 forcing; (b) global mean temperature (K) and NAMOC index (Sv); (c) cumulative Greenland contribution to global mean sea level rise; and (d) mass balance (MB) contribution to global mean sea level rise and components of the mass budget (SMB, Ice Discharge) with right axis: Gt year^{-1}, left axis: mm year^{-1} . The blue-shaded areas denote the mid-century (2031–2050, left), and end-of-century (2081–2100, right) periods.

of century (Table S1). The associated SLR is 23-mm SLE by 2050 and 109-mm SLE by 2100. Estimates of 2003–2013 Greenland mass loss from the Gravity Recovery and Climate Experiment satellite mission range from 0.77- to 0.79-mm SLE year^{-1} (Ran et al., 2018; Schrama et al., 2014; Velicogna et al., 2014). The simulated SLR in the contemporary period is underestimated, likely for several reasons. First, a substantial part of the observed mass loss is attributed to ocean forcing (Wood et al., 2018), which is missing in the model. Second, anomalous atmospheric circulation, in particular blocking over Greenland, has contributed to the observed mass loss but is not simulated correspondingly in global climate models (Delhasse et al., 2018; Hanna et al., 2018). Other model biases (e.g., initial ice sheet topography) can explain the remaining differences. The temperature change at the time of mass loss acceleration is approximately 2.7 K with respect to preindustrial. By 2100, the simulated GrIS area and volume decrease by 3% and 1.2%, respectively, compared to the preindustrial ice sheet.

The SMB is the main contributor to GrIS mass loss (Figure 1d, Table S1). By mid-century, the GrIS-integrated SMB is still positive (350 Gt year^{-1}) and 214 Gt year^{-1} lower than in the contemporary period. Based on a linear, long-term trend, the integrated SMB becomes negative by 2077. The expansion of ablation areas (i.e., areas with average SMB < 0) accelerates with similar timing. By mid-century, the SMB is strongly reduced in southern Greenland (Figure S1), and by end of century, the ablation areas extend far inland around the entire ice sheet, including the northern periphery. At the northern margins, the ablation zone advances later, and progresses faster inland, than at the southern margins. By end of century the northern surface mass loss also has intensified. In the ice sheet interior, the SMB moderately increases due to greater snowfall.

As the SMB becomes more negative, the ice sheet thins (Figures S1b–S1c). Most of the thinning occurs in the south and below the 2000-m elevation contour, while the ice sheet interior moderately thickens (Figures S1e–S1f). Surface velocities increase in the intermediate areas between the high interior and the ice sheet margins (Figures S1h–S1i) where the surface is steeper because of SMB-induced margin thinning. Conversely, surface velocities decrease at the thinner margins. As a result, total ice discharge is reduced by 8% (45 Gt year^{-1}) at mid-century and by 33% (189 Gt year^{-1}) at end of century compared to the contemporary period (Table S1 and Figure S2). The reduced discharge partly compensates for the mass loss due to more negative SMB (214 and 1,129 Gt year^{-1} at mid-century and end of century, respectively; see Table S1).

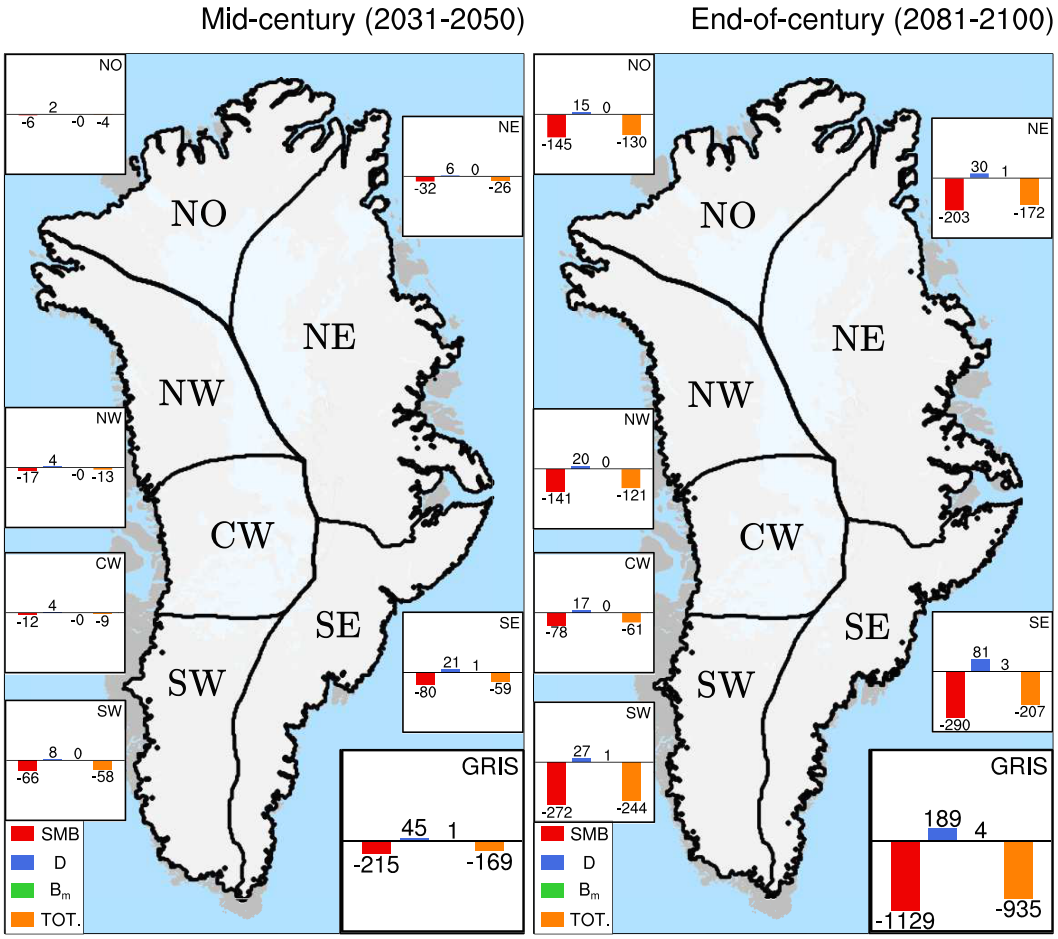

Figure 2. Change in GrIS mass balance (TOT) and components with respect to the contemporary budget (1995–2014) for mid-century (2031–2050, left), and end of century (2081–2100, right), in Gt year^{-1}. GrIS mass balance (TOT; orange) = surface mass balance (SMB; red) - ice discharge (D; blue) - basal melt (B_m; green). Note that ice discharge and basal melt are defined negative here for graphical purposes.

3.2. Sea Level Rise Contribution by Drainage Basin

This section presents mid-century and end-of-century mass balance changes for individual drainage basins, with the contemporary mass budget as a reference (Figure S3). Text S3 gives a brief comparison of simulated and observed outlet glacier ice discharge (Enderlin et al., 2014).

By mid-century, the mean total GrIS mass loss is 169 Gt year^{-1} (Figure 2), as the result of an SMB decrease partly offset by reduced ice discharge. In all six drainage basins the SMB decreases but remains positive (Figure S3), with the largest reductions in the SW (66 Gt year^{-1}) and SE (80 Gt year^{-1}), there is a modest mid-century decrease in the NE basin (32 Gt year^{-1}), with smaller reductions in the CW, NW, and NO basins. Taken together, the SMB in the northern basins (NO, NW, NE) decreases by 55 Gt year^{-1} or about 26% of the six basin total.

At the end of the century (right panel in Figure 2), the mean mass budget of the GrIS has decreased by 935 Gt year^{-1} compared to the contemporary budget, and the total surface mass balance is reduced by 1,129 Gt year^{-1}. The mass loss from ice discharge is reduced by 189 Gt year^{-1}, partly (17%) canceling the surface mass loss. The largest end of century decreases in SMB (290 Gt year^{-1}) and ice discharge (81 Gt year^{-1}) are in the SE basin, which make the second largest SLR contribution (215 Gt year^{-1}; right panel in Figure S3). The SW basin, with the next largest SMB decrease (272 Gt year^{-1}) and a smaller reduction in discharge (27 Gt year^{-1}), is the largest net contributor to SLR (235 Gt year^{-1}). The three northern basins also have large SMB decreases: 203, 145, and 141 Gt year^{-1}, respectively, for the NE, NO, and NW basins. Together, the northern basins contribute 43% of the total end-of-century SMB decrease and 45% of the total SLR.

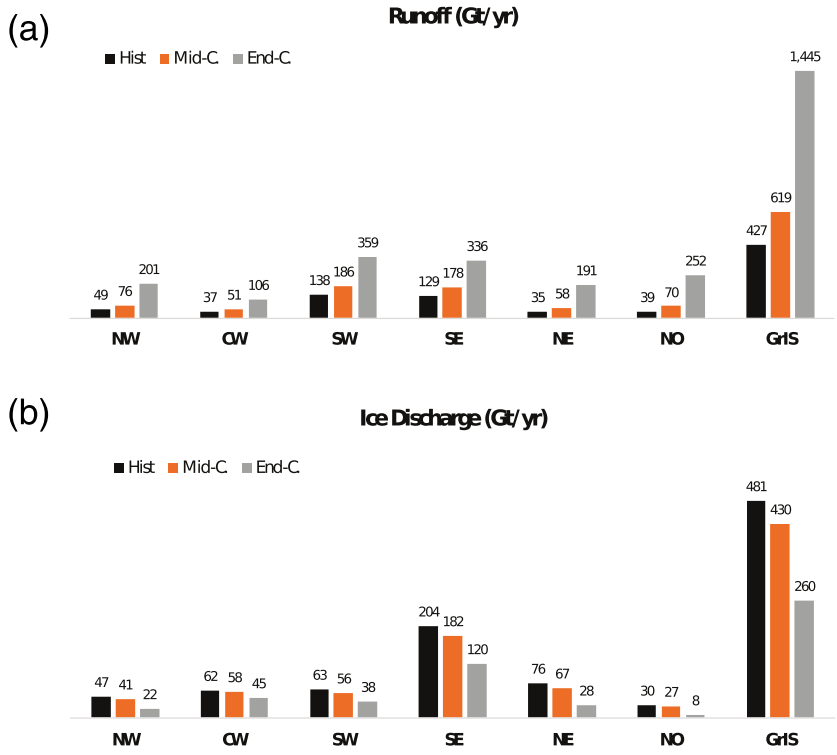

Figure 3. Freshwater flux (Gt year^{-1}) from (a) Greenland runoff and (b) ice discharge per basin for the contemporary, mid-century and end-of-century periods.

3.3. Freshwater Fluxes

This section presents the mid-century and end-of-century freshwater fluxes to the ocean from individual drainage basins (Figure 3). The change in total freshwater fluxes is moderate at mid-century, with runoff increasing by less than 200 Gt year^{-1} (from 427 to 619 Gt year^{-1}), and a small decrease in the solid flux (i.e., ice discharge), from 481 to 430 Gt year^{-1} (Figure 3). By this time, the NAMOC has already decreased by 6 Sv (Figure 1), suggesting that increased Greenland freshwater fluxes play only a minor role in weakening the NAMOC.

By end of century, runoff has more than tripled compared to the contemporary period, increasing to 1,445 Gt year^{-1} (Figure 3). The reduced ice discharge (260 Gt year^{-1}) results in a total freshwater flux that is not quite double the contemporary flux (1,705 Gt year^{-1} compared to 908). Per basin, the SW and SE regions contribute the most to the total runoff during all periods. However, their relative contribution decreases from 63% in the contemporary period to 48% at end of century. Thanks to a large increase in runoff, the relative freshwater contribution from the northern basins (NW, NE, and NO) increases from 29% in the contemporary period to 44% at end of century.

Throughout the simulation, the SE region has the largest GrIS ice discharge in absolute terms (Figure 3). Relative to the contemporary discharge, all basins have similar reductions of around 10% at mid-century, but by end of century the northern basins have the greatest reductions (62%).

3.4. Comparison to CESM2 Simulations Without an Interactive Greenland Ice Sheet

Finally, we compare the SMB and NAMOC responses to the historical ensembles and a suite of scenario simulations conducted using CESM2.1 without an interactive GrIS but with the same SEB-based SMB calculation. We consider 11 ensemble members from the historical period and the following scenario simulations between 2015 and 2100: SSP1-2.6 (two members), SSP2-4.5 (three members), SSP3-7.0 (two members), and SSP5-8.5 (two members), with scenario details provided by O'Neill et al. (2016).

Compared to CESM2.1-CISM2.1, the CESM2.1 simulations have a lower contemporary and end-of-century SMB and a greater SMB sensitivity to warming (Figure 4 and Table S3). Also, the reduction in SMB between the full historical mean (1850–2014) and the contemporary mean (1995–2014) is larger in CESM2.1 (65 Gt

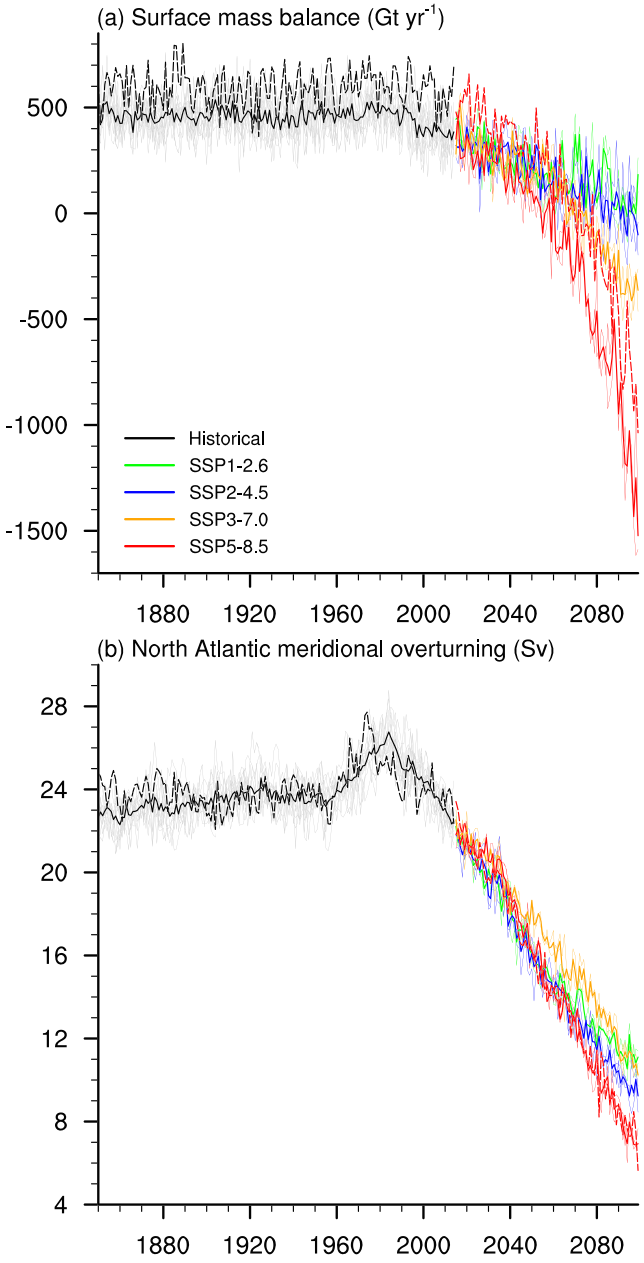

Figure 4. Comparison of evolution of (a) SMB (Gt year^{-1}) and (b) NAMOC index (Sv) for the historical (black, dashed) and SSP5-8.5 (red, dashed) coupled simulations in this paper versus CESM2.1 historical (black, solid) and scenario simulations (solid) with a prescribed surface elevation, nondynamical Greenland Ice Sheet (that is, with nonevolving CISM2.1). Thick lines represent CESM2.1 scenario ensemble means.

year^{-1}, from 455 to 390 Gt year^{-1}) than in CESM2.1-CISM2.1 (17 Gt year^{-1}, from 588 to 571 Gt year^{-1}). The contemporary CESM2.1-CISM2.1 overestimates the SMB (Noël et al., 2018). Also, there is higher interannual SMB variability than CESM2.1 (80 Gt year^{-1} vs. 28 Gt year^{-1}, Table S3). These differences are, at least in part, because the SMB is calculated over a different ice sheet topography. CESM2.1 simulates a realistic SMB for the contemporary period (Noël et al., 2019).

At end of century under SSP5-8.5 forcing, the SMB is almost 400 Gt year^{-1} lower in CESM2.1 compared to CESM2.1-CISM2.1 (−906 vs. −511 Gt year^{-1}). The smaller SMB reduction in CESM2.1-CISM2.1 is likely the result of dynamic removal of high-melt areas on the margins. These areas are allowed to remain in the nonevolving CESM2.1 simulation, favoring an overestimate of SMB decline. The CESM2.1-CISM2.1

response to SSP5-8.5 does, however, exceeds the CESM2.1 response to less extreme scenarios, including SSP3-7.0. Despite the differences in SMB magnitude, the timing of SMB evolution in the two models is similar for SSP5-8.5.

NAMOC evolution also is similar in CESM2.1-CISM2.1 and CESM2.1 simulations (Figure 4 and Table S3). The peak NAMOC strength in the second half of the 20th century, mentioned in section 3.1, is present in both simulations. Generally, the NAMOC in CESM2 is sensitive to external forcing in the 21st century, with large reductions in all scenarios including SSP1-2.6. In the SSP5-8.5 projections, there is no discernible differences in NAMOC weakening between simulations with and without dynamical GrIS.

4. Discussion and Conclusions

This study presents the first simulations performed with CESM2.1-CISM2.1 including an interactive Greenland Ice Sheet. The projected GrIS contribution to SLR by 2100 in the SSP5-8.5 scenario is 109 mm, in general agreement with pre-AR5 multimodel results (Bindschadler et al., 2013) and the AR5 assessment (Church et al., 2013). The latter gives a likely range of 70 to 210 mm. Our projection also lies within the range of post-AR5 estimates from Fürst et al. (2015), Calov et al. (2018), and Golledge et al. (2019), which are of 102 ± 32, 46–130, and 112 mm, respectively. Vizcaino et al. (2015) gave a lower estimate (58 mm), based on a coupled Earth system/ice sheet model of coarse resolution (3.75°) with an energy-balance-based melt calculation. Aschwanden et al. (2019) estimated a higher range of 140–330 mm, using an ice sheet model forced with spatially uniform warming. In our projection, the negative SMB trend increases sharply at mid-century, so that most of the SLR contribution is after 2050.

This study projects an increased contribution of the northern basins to total GrIS mass loss after mid-century, in agreement with previous studies. Noël et al. (2019) found a 46% expansion of ablation area in northern Greenland between the early 1990s and 2017, almost twice as much as in the south, because runoff in the north and northeast increased relative to the total runoff due to longer exposure of bare ice. The high response in the north is also explained by the relatively wide ablation zones from low surface slopes (Van den Broeke et al., 2016). In 21st century RCP4.5 and RCP8.5 projections with the regional climate model MAR with static GrIS topography, Tedesco and Fettweis (2012) also found a high sensitivity of SMB to higher temperatures in the north. Similarly, Lenaerts et al. (2015), in a 21st century RCP4.5 projection with the regional climate model RACMO, projected a strongly nonlinear response of runoff in northern and northeastern Greenland, in connection with low meltwater buffering capacity of the snow pack.

Acknowledgments
CESM2 is an open source model, available at https://www.cesm.ucar.edu/. The CESM project is supported primarily by the National Science Foundation (NSF). This material is based upon work supported by the National Center for Atmospheric Research, which is a major facility sponsored by the NSF under Cooperative Agreement 1852977. Computing and data storage resources, including the Cheyenne supercomputer (doi:10.5065/D6RX99HX), were provided by the Computational and Information Systems Laboratory (CISL) at NCAR. The World Climate Research Program (WGCM) Infrastructure Panel is the official CMIP document home: https://www.wcrp-climate.org/wgcm-cmip. The CMIP6 and ISMIP6 simulations are freely available and accessible via the Earth System Grid Federation (ESGF) data portals https://esgf.llnl.gov/nodes.html. We thank the Climate and Cryosphere (CliC) project, which provided support for ISMIP6 through sponsoring of workshops, hosting the ISMIP6 website and wiki, and promoting ISMIP6. This is ISMIP6 Contribution No. 19. LM, MP, MV, and CES acknowledge funding from the European Research Council (Grant ERC-StG-678145-CoupledIceClim). RS acknowledges funding from the Dutch Research Council (NWO Grant ALWOP.2015.096).

References

Aschwanden, A., Fahnestock, M. A., Truffer, M., Brinkerhoff, D. J., Hock, R., Khroulev, C., et al. (2019). Contribution of the Greenland Ice Sheet to sea level over the next millennium. *Science Advances*, *5*(6), eaav9396. https://doi.org/10.1126/sciadv.aav9396

Bamber, J. L., Oppenheimer, M., Kopp, R. E., Aspinall, W. P., & Cooke, R. M. (2019). Ice sheet contributions to future sea-level rise from structured expert judgment. *Proceedings of the National Academy of Sciences*, *116*(23), 11,195–11,200. https://doi.org/10.1073/pnas.1817205116

Bauer, E., & Ganopolski, A. (2017). Comparison of surface mass balance of ice sheets simulated by positive-degree-day method and energy balance approach. *Climate of the Past*, *13*(7), 819–832. https://doi.org/10.5194/cp-13-819-2017

Bindschadler, R. A., Nowicki, S., Abe-Ouchi, A., Aschwanden, A., Choi, H., Fastook, J., et al. (2013). Ice-sheet model sensitivities to environmental forcing and their use in projecting future sea level (the SeaRISE project). *Journal of Glaciology*, *59*(214), 159–244. https://doi.org/10.3189/2013JoG12J125

Born, A., Imhof, M. A., & Stocker, T. F. (2019). An efficient surface energy–mass balance model for snow and ice. *The Cryosphere*, *13*(5), 1529–1546. https://doi.org/10.5194/tc-13-1529-2019

Bougamont, M., Bamber, J. L., Ridley, J. K., Gladstone, R. M., Greuell, W., Hanna, E., et al. (2007). Impact of model physics on estimating the surface mass balance of the Greenland ice sheet. *Geophysical Research Letters*, *34*, L17501. https://doi.org/10.1029/2007GL030700

Calov, R., Beyer, S., Greve, R., Beckmann, J., Willeit, M., Kleiner, T., et al. (2018). Simulation of the future sea level contribution of Greenland with a new glacial system model. *The Cryosphere*, *12*(10), 3097–3121. https://doi.org/0.5194/tc-12-3097-2018

Chen, X., Zhang, X., Church, J. A., Watson, C. S., King, M. A., Monselesan, D., et al. (2017). The increasing rate of global mean sea-level rise during 1993–2014. *Nature Climate Change*, *7*(7), 492–495. https://doi.org/10.1038/nclimate3325

Church, J. A., Clark, P. U., Cazenave, A., Gregory, J. M., Jevrejeva, S., Levermann, A., et al. (2013). Sea level change. In T. F. Stocker, D. Qin, G.-K. Plattner, M. Tignor, S.K. Allen, et al. (Eds.), *Climate change 2013: The physical science basis. Contribution of working group i to the fifth assessment report of the intergovernmental panel on climate change* (pp. 1137–1216). Cambridge, United Kingdom and New York, NY, USA: Cambridge University Press. www.climatechange2013.org

Dai, A., Luo, D., Song, M., & Liu, J. (2019). Arctic amplification is caused by sea-ice loss under increasing CO2. *Nature Communications*, *10*(1), 121. https://doi.org/10.1038/s41467-018-07954-9

Danabasoglu, G., Bates, S. C., Briegleb, B. P., Jayne, S. R., Jochum, M., Large, W. G., et al. (2012). The CCSM4 ocean component. *Journal of Climate*, *25*(5), 1361–1389. https://doi.org/10.1175/JCLI-D-11-00091.1

Danabasoglu, G., Lamarque, J.-F., Bacmeister, J., Bailey, D. A., DuVivier, A. K., Edwards, J., et al. (2020). The Community Earth System Model version 2 (CESM2). *Journal of Advances in Modeling Earth Systems*, *12*, e2019MS001916. https://doi.org/10.1029/2019MS001916

Delhasse, A., Fettweis, X., Kittel, C., Amory, C., & Agosta, C. (2018). Brief communication: Impact of the recent atmospheric circulation change in summer on the future surface mass balance of the Greenland Ice Sheet. *The Cryosphere*, *12*(11), 3409–3418. https://doi.org/10.5194/tc-12-3409-2018

Enderlin, E. M., Howat, I. M., Jeong, S., Noh, M.-J., Van Angelen, J. H., & Van den Broeke, M. R. (2014). An improved mass budget for the Greenland ice sheet. *Geophysical Research Letters*, *41*, 866–872. https://doi.org/10.1002/2013GL059010

Eyring, V., Bony, S., Meehl, G. A., Senior, C. A., Stevens, B., Stouffer, R. J., & Taylor, K. E. (2016). Overview of the Coupled Model Intercomparison Project Phase 6 (CMIP6) experimental design and organization. *Geoscientific Model Development*, *9*(5), 1937–1958. https://doi.org/10.5194/gmd-9-1937-2016

Frajka-Williams, E., Ansorge, I. J., Baehr, J., Bryden, H. L., Chidichimo, M. P., Cunningham, S. A., et al. (2019). Atlantic meridional overturning circulation: Observed transport and variability. *Frontiers in Marine Science*, *6*, 260. https://doi.org/10.3389/fmars.2019.00260

Fürst, J. J., Goelzer, H., & Huybrechts, P. (2015). Ice-dynamic projections of the Greenland ice sheet in response to atmospheric and oceanic warming. *The Cryosphere*, *9*(3), 1039–1062. https://doi.org/10.5194/tc-9-1039-2015

Fyke, J., Sergienko, O., Lofverstrom, M., Price, S., & Lenaerts, JanT. M. (2018). An overview of interactions and feedbacks between ice sheets and the Earth system. *Reviews of Geophysics*, *56*, 361–408. https://doi.org/10.1029/2018RG000600

Fyke, J. G., Weaver, A. J., Pollard, D., Eby, M., Carter, L., & Mackintosh, A. (2011). A new coupled ice sheet/climate model: Description and sensitivity to model physics under Eemian, Last Glacial Maximum, late Holocene and modern climate conditions. *Geoscientific Model Development*, *4*(1), 117–136. https://doi.org/10.5194/gmd-4-117-2011

Goelzer, H., Robinson, A., Seroussi, H., & Van de Wal, R. S. W. (2017). Recent progress in Greenland ice sheet modelling. *Current Climate Change Reports*, *3*(4), 291–302. https://doi.org/10.1007/s40641-017-0073-y

Golledge, N. R., Keller, E. D., Gomez, N., Naughten, K. A., Bernales, J., Trusel, L. D., & Edwards, T. L. (2019). Global environmental consequences of twenty-first-century ice-sheet melt. *Nature*, *566*(7742), 65–72. https://doi.org/10.1038/s41586-019-0889-9

Graversen, R. G., Drijfhout, S., Hazeleger, W., Van de Wal, R., Bintanja, R., & Helsen, M. (2011). Greenland's contribution to global sea-level rise by the end of the 21st century. *Climate Dynamics*, *37*(7), 1427–1442. https://doi.org/10.1007/s00382-010-0918-8

Hanna, E., Fettweis, X., & Hall, R. J. (2018). Brief communication: Recent changes in summer Greenland blocking captured by none of the CMIP5 models. *The Cryosphere*, *12*(10), 3287–3292. https://doi.org/10.5194/tc-12-3287-2018

Hunke, E., Lipscomb, W., Jones, P., Turner, A., Jeffery, N., & Elliott, S. (2017). CICE, The Los Alamos Sea Ice Model, Version 00. https://www.osti.gov//servlets/purl/1364126

Huybrechts, P., Goelzer, H., Janssens, I., Driesschaert, E., Fichefet, T., Goosse, H., & Loutre, M.-F. (2011). Response of the Greenland and Antarctic ice sheets to multi-millennial greenhouse warming in the Earth system model of intermediate complexity LOVECLIM. *Surveys in Geophysics*, *32*(4), 397–416. https://doi.org/10.1007/s10712-011-9131-5

Joughin, I., Smith, B., Howat, I., & Scambos, T. (2015). MEaSUREs Greenland Ice Sheet Velocity Map from InSAR Data, Version 2. National Snow and Ice Data Center, Boulder, Colorado USA.

Joughin, I., Smith, B., Howat, I., Scambos, T., & Moon, T. (2010). Greenland flow variability from ice-sheet-wide velocity mapping. *Journal of Glaciology*, *56*(197), 415–430.

Krapp, M., Robinson, A., & Ganopolski, A. (2017). SEMIC: An efficient surface energy and mass balance model applied to the Greenland ice sheet. *The Cryosphere*, *11*(4), 1519–1535. https://doi.org/10.5194/tc-11-1519-2017

Lawrence, D. M., Fisher, R. A., Koven, C. D., Oleson, K. W., Swenson, S. C., Bonan, G., et al. (2019). The Community Land Model version 5: Description of new features, benchmarking, and impact of forcing uncertainty. *Journal of Advances in Modeling Earth Systems*, *11*, 4245–4287. https://doi.org/10.1029/2018MS001583

Le clec'h, S., Charbit, S., Quiquet, A., Fettweis, X., Dumas, C., Kageyama, M., et al. (2019). Assessment of the Greenland ice sheet–atmosphere feedbacks for the next century with a regional atmospheric model coupled to an ice sheet model. *The Cryosphere*, *13*(1), 373–395. https://doi.org/10.5194/tc-13-373-2019

Leguy, G., Lipscomb, W. H., & Sacks, W. J. (2018). CESM land ice documentation and user guide. National Centers for Atmospheric Research, Boulder, https://escomp.github.io/cism-docs/cism-in-cesm/versions/master/html/index.html

Lenaerts, J. T. M., Le Bars, D., Van Kampenhout, L., Vizcaino, M., Enderlin, E. M., & Van den Broeke, M. R. (2015). Representing Greenland ice sheet freshwater fluxes in climate models. *Geophysical Research Letters*, *42*, 6373–6381. https://doi.org/10.1002/2015GL064738

Li, H.-Y., Leung, L. R., Getirana, A., Huang, M., Wu, H., Xu, Y., et al. (2015). Evaluating global streamflow simulations by a physically based routing model coupled with the community land model. *Journal of Hydrometeorology*, *16*(2), 948–971. https://doi.org/10.1175/JHM-D-14-0079.1

Lipscomb, W. H., Fyke, J. G., Vizcaino, M., Sacks, W. J., Wolfe, J., Vertenstein, M., et al. (2013). Implementation and initial evaluation of the glimmer community ice sheet model in the community earth system model. *Journal of Climate*, *26*(19), 7352–7371. https://doi.org/10.1175/JCLI-D-12-00557.1

Lipscomb, W. H., Price, S. F., Hoffman, M. J., Leguy, G. R., Bennett, A. R., Bradley, S. L., et al. (2019). Description and evaluation of the Community Ice Sheet Model (CISM) v2.1. *Geoscientific Model Development*, *12*(1), 387–424. https://doi.org/10.5194/gmd-12-387-2019

Mikolajewicz, U., Vizca-Ino, M., Jungclaus, J., & Schurgers, G. (2007). Effect of ice sheet interactions in anthropogenic climate change simulations. *Geophysical Research Letters*, *34*, L18706. https://doi.org/10.1029/2007GL031173

Noël, B., Van Kampenhout, L., Van de Berg, W. J., Lenaerts, J. T. M., Wouters, B., & Van den Broeke, M. R. (2019). Brief communication: CESM2 climate forcing (1950–2014) yields realistic Greenland ice sheet surface mass balance. *The Cryosphere Discussions*, *2019*, 1–17. https://doi.org/10.5194/tc-2019-209

Noël, B., Van de Berg, W. J., Lhermitte, S., & Van den Broeke, M. R. (2019). Rapid ablation zone expansion amplifies north Greenland mass loss. *Science Advances*, *5*(9), 1–9. https://doi.org/10.1126/sciadv.aaw0123

Noël, B., Van de Berg, W. J., Van Wessem, J. M., Van Meijgaard, E., Van As, D., Lenaerts, J. T. M., et al. (2018). Modelling the climate and surface mass balance of polar ice sheets using RACMO2 – Part 1: Greenland (1958–2016). *The Cryosphere*, *12*(3), 811–831. https://doi.org/10.5194/tc-12-811-2018

Nowicki, S. M. J., Payne, A., Larour, E., Seroussi, H., Goelzer, H., Lipscomb, W., et al. (2016). Ice Sheet Model Intercomparison Project (ISMIP6) contribution to CMIP6. *Geoscientific Model Development*, *9*(12), 4521–4545. https://doi.org/10.5194/gmd-9-4521-2016

O'Neill, B. C., Tebaldi, C., Van Vuuren, D. P., Eyring, V., Friedlingstein, P., Hurtt, G., et al. (2016). The Scenario Model Intercomparison Project (ScenarioMIP) for CMIP6. *Geoscientific Model Development*, *9*(9), 3461–3482. https://doi.org/10.5194/gmd-9-3461-2016

Rae, J. G. L., Adalgeirsdottirr, G., Edwards, T. L., Fettweis, X., Gregory, J. M., Hewitt, H. T., et al. (2012). Greenland ice sheet surface mass balance: Evaluating simulations and making projections with regional climate models. *The Cryosphere*, *6*(6), 1275–1294. https://doi.org/10.5194/tc-6-1275-2012

Ran, J., Vizcaino, M., Ditmar, P., Van den Broeke, M. R., Moon, T., Steger, C. R., et al. (2018). Seasonal mass variations show timing and magnitude of meltwater storage in the Greenland Ice Sheet. *The Cryosphere*, *12*(9), 2981–2999. https://doi.org/10.5194/tc-12-2981-2018

Ridley, J. K., Huybrechts, P., Gregory, J. M., & Lowe, J. A. (2005). Elimination of the Greenland ice sheet in a high CO2 climate. *Journal of Climate*, *18*(17), 3409–3427. https://doi.org/10.1175/JCLI3482.1

Rignot, E., & Mouginot, J. (2012). Ice flow in Greenland for the international polar year 2008–2009. *Geophysical Research Letters*, *39*, L11501. https://doi.org/10.1029/2012GL051634

Ruckamp, M., Greve, R., & Humbert, A. (2019). Comparative simulations of the evolution of the Greenland ice sheet under simplified Paris Agreement scenarios with the models SICOPOLIS and ISSM. *Polar Science*, *21*, 14–25. https://doi.org/10.1016/j.polar.2018.12.003

Schrama, ErnstJ. O., Wouters, B., & Rietbroek, R. (2014). A mascon approach to assess ice sheet and glacier mass balances and their uncertainties from GRACE data. *Journal of Geophysical Research: Solid Earth*, *119*, 6048–6066. https://doi.org/10.1002/2013JB010923

Sellevold, R., Van Kampenhout, L., Lenaerts, J. T. M., Noël, B., Lipscomb, W. H., & Vizcaino, M. (2019). Surface mass balance downscaling through elevation classes in an Earth System Model: Analysis, evaluation and impacts on the simulated climate. *The Cryosphere Discussions*, *2019*, 1–25. https://doi.org/10.5194/tc-2019-122

Shepherd, A., Ivins, E., Rignot, E., Smith, B., Van den Broeke, M., Velicogna, I., et al. (2019). Mass balance of the Greenland Ice Sheet from 1992 to 2018. *Nature*, *579*, 233–239. https://doi.org/10.1038/s41586-019-1855-2

Smith, R., Jones, P., Briegleb, B., Bryan, F., Danabasoglu, G., Dennis, J., et al. (2010). The parallel ocean program (POP) reference manual: Ocean component of the community climate system model (CCSM). LANL, Tech. Report, LAUR-10-01853.

Sun, Q., Whitney, M. M., Bryan, F. O., & heng Tseng, Y. (2017). A box model for representing estuarine physical processes in Earth system models. *Ocean Modelling*, *112*, 139–153. https://doi.org/10.1016/j.ocemod.2017.03.004

Tedesco, M., & Fettweis, X. (2012). 21st century projections of surface mass balance changes for major drainage systems of the Greenland ice sheet. *Environmental Research Letters*, *7*(4), 045,405. https://doi.org/10.1088/1748-9326/7/4/045405

Van den Broeke, M. R., Enderlin, E. M., Howat, I. M., Kuipers Munneke, P., Noël, B. P. Y., Van de Berg, W. J., et al. (2016). On the recent contribution of the Greenland ice sheet to sea level change. *The Cryosphere*, *10*(5), 1933–1946. https://doi.org/10.5194/tc-10-1933-2016

Van den Broeke, M., Smeets, P., Ettema, J., & Munneke, P. K. (2008). Surface radiation balance in the ablation zone of the west Greenland ice sheet. *Journal of Geophysical Research*, *113*, D13105. https://doi.org/10.1029/2007JD009283

Velicogna, I., Sutterley, T. C., & Van den Broeke, M. R. (2014). Regional acceleration in ice mass loss from Greenland and Antarctica using GRACE time-variable gravity data. *Geophysical Research Letters*, *41*, 8130–8137. https://doi.org/10.1002/2014GL061052

Vizcaino, M. (2014). Ice sheets as interactive components of Earth System Models: Progress and challenges. *Wiley Interdisciplinary Reviews: Climate Change*, *5*(4), 557–568. https://doi.org/10.1002/wcc.285

Vizcaino, M., Mikolajewicz, U., Gröger, M., Maier-Reimer, E., Schurgers, G., & Winguth, ArneM. E. (2008). Long-term ice sheet–climate interactions under anthropogenic greenhouse forcing simulated with a complex Earth System Model. *Climate Dynamics*, *31*(6), 665–690. https://doi.org/10.1007/s00382-008-0369-7

Vizcaino, M., Mikolajewicz, U., Ziemen, F., Rodehacke, C. B., Greve, R., & Van den Broeke, M. R. (2015). Coupled simulations of Greenland Ice Sheet and climate change up to A.D. 2300. *Geophysical Research Letters*, *42*, 3927–3935. https://doi.org/10.1002/2014GL061142

Wood, M., Rignot, E., Fenty, I., Menemenlis, D., Millan, R., Morlighem, M., et al. (2018). Ocean-induced melt triggers glacier retreat in Northwest Greenland. *Geophysical Research Letters*, *45*, 8334–8342. https://doi.org/10.1029/2018GL078024